



## ORIGINAL ARTICLE

# Theoretical and Experimental Analysis for the Removal of Dye from Aqueous Solution by Using Charcoal from Pomegranate Seeds

Lekaa Hussain Khadim

Department of Chemistry, College of Education for Woman, University of Kufa, Iraq

Received: 17 September 2021

Accepted: 5 March 2022

**KEYWORDS**

Dyes;  
Activated charcoal;  
DFT;  
Adsorption;  
Isotherms;  
Adsorption Kinetic

**ABSTRACT:** This study initiates an experimental and theoretical investigation to evaluate the selective and competitive adsorption of two dyes, sulforhodamine B and Brilliant Green, on coal from pomegranate seeds. For this purpose, the effects of numerous parameters like initial dye concentration, initial pH, adsorbent dose and solution temperature were examined and studied in batch mode. The experimental results indicate that the adsorption is fast and fits better with the quasi-second order kinetic model than the quasi-first order kinetics. Adsorption data were studied using Langmuir and Freundlich isotherms. The obtained results showed that the Freundlich model provided a better correlation of the experimental data. The geometries of sulforhodamine B and Brilliant Green were optimized using Gaussian 09W software through the density functional theory (DFT) at the theoretical level B3LYP / LanL2DZ, and the calculations (link length and connection angle) were well matched with experimental data at both levels.

**INTRODUCTION**

According to the research conducted in the 70s, one of the sources of environmental pollution was organic solvents used in chemical industries, especially paint and resin industries and related industries. Organic compounds accelerate the photochemical synthesis of ozone in the layers near the earth and cause the formation of ozone in the lower layers of the atmosphere, which is very dangerous for humans and other creatures. Following the international meetings and the approval of laws regarding the permissible level of environmental pollution, in the 80s, moving towards new methods of applying paint and preparing new environmentally friendly compounds was put on the agenda of paint industry research centers.

Dyes are colored organic chemicals found in wastewater from a variety of industries, including paper, textiles, leather, cosmetics and printing. If the release of these

dyes has a long-term negative effect on the environment, the color of water. It is not recommended to drink and use at home. Dye molecules are usually composed of complex aromatic rings and have bright colors. This aromaticity indicates long-term stability against biodegradation [1, 2]. Furthermore, dyes released in natural water sources not only reduce the amount of oxygen dissolved in water, but also affect the stability of the ecosystem [3-5]. This results in significant amounts of colored wastewater [6]. Consequently, it is very significant to develop effective approaches for removing dyes from aqueous media. Photocatalytic degradation [7, 8], cation exchange membranes [9], electrochemical [10], aggregation [11] and activated carbon adsorption [12, 13] are some of the chemical and physical dyeing methods used for color removal from the paint wastewater. The adsorption method is used to treat

\*Corresponding author: liqaa.aljailawi@uokufa.edu.iq (L. Hussain Khadim)  
DOI: 10.22034/jchr.2022.694637

hazardous wastewater, and activated carbon is expensive, but widely used to remove various pollutants. As a result, low-cost additional materials, such as residual biomass, a renewable crop that are biodegradable at the lowest acceptable cost associated, have been proposed as substitutes and have excellent adsorption features for contaminants, metals or compounds. The principle of activated carbon in plants is a versatile adsorbent with great economic benefits for human waste or water treatment for industrial purposes [14]. Pollution-free recovery of agricultural waste is a major challenge and is recommended for sustainable industrial development for the conservation of the natural environment. All low-cost materials, such as biomass waste: apple peels [15], date seeds [16], olive seeds [17], peach seeds [18], pomegranate peels [19], grains coffee [20], coffee grounds [[21]], carbonated tea waste [22], mud [23], coconut shells [24] and apricots with seeds [25] may be used as precursors for the production of activated carbon. The aim of this study is to explore the possibility of using charcoal obtained from pomegranate seeds to remove some dyes from aqueous solutions, such as sulforodamine B and bright green. This study includes the optimization of the maximum adsorption conditions by investigating the impact of several parameters, like the adsorbent dose, initial concentration, the temperature and pH of the solution and the determination of the adsorption isotherms.

## MATERIALS AND METHODS

### Methods

#### Settings and Computational details

Structural calculations of dyes were performed using DFT. The simulations were performed in the gaseous state by approximating the isolated molecules using the Gaussian luxury 09 W used in all calculations in this study [26]. Gaussian output files were viewed using Gaussian View 05 software [27]. The dye geometry was optimized using the functional density theory (DFT) at B3LYP / LANL2DZ. The most common parameter that has a significant impact is chemical reactivity. Own values of the highest occupancy molecular orbital energy (EHOMO), lowest occupied molecular orbital energy

(ELUMO), energy gap (EGAP), global electrophilicity index ionization energy (IE), global hardness ( $\eta$ ), global softness (S), and electronic affinity (EA) [28].

$$IE = -E_{HOMO}$$

$$EA = -E_{LUMO}$$

EGAP is the difference between the (EHOMO) and (ELUMO).

$$\Delta E \text{ gap} = E_{LUMO} - E_{HOMO}$$

The parameter of ( $\eta$ ) was obtained according to the equation:

$$\eta = \frac{I - A}{2} = \frac{EHOMO - ELUMO}{2}$$

The parameter of (S), was obtained according to the equation:

$$S = \frac{1}{\eta} = \frac{2}{EHOMO - ELUMO}$$

The electronegativity was calculated according to the equation:

$$\chi = \frac{I + A}{2} = \frac{-(ELUMO - EHOMO)}{2}$$

The electronic chemical potential ( $\mu$ ) was calculated from the molecular orbital energies as follows [29].

$$\mu = \frac{ELUMO + EHOMO}{2}$$

### Experimental study

#### Preparation of surface

Charcoal obtained from pomegranate seeds was prepared by washing the seeds several times with distilled water, drying them at (100) C and placing them in an anaerobic oven (500 C) for 2 hours. Take aeration charcoal (CRH) and finely grind the charcoal. After sieving with a sieve with a diameter of 0, 1  $\mu$  m, wash several times with distilled water and dry at a temperature of (50°C) for 2 hours. (all)

#### Preparation of dyes solutions and calibration curve

As a representative cationic dye, a dye with a purity of 99% was purchased from Sigma-Aldrich and used without further purification. A standard solution (500 ml) of the three dyes was dissolved in distilled water weighing 0.1g to prepare a concentration (200 ppm).

Then, different concentrations were prepared varying (1-10 ppm). The wavelength  $\lambda_{max}$  was measured using distilled water to obtain the maximum absorption of the dye (Note) (control). The absorbance for each of the ten samples was then measured with a UV-Vis spectrophotometer to determine the dye calibration

curve. The calibration curve is plotted for dilute solutions, and the linearity of the calibration curve is a good indication that the calibration curve follows Beer's law. (Behr-Lambert) is as shown in Figure. Table 1 shows the selected features of these dyes.

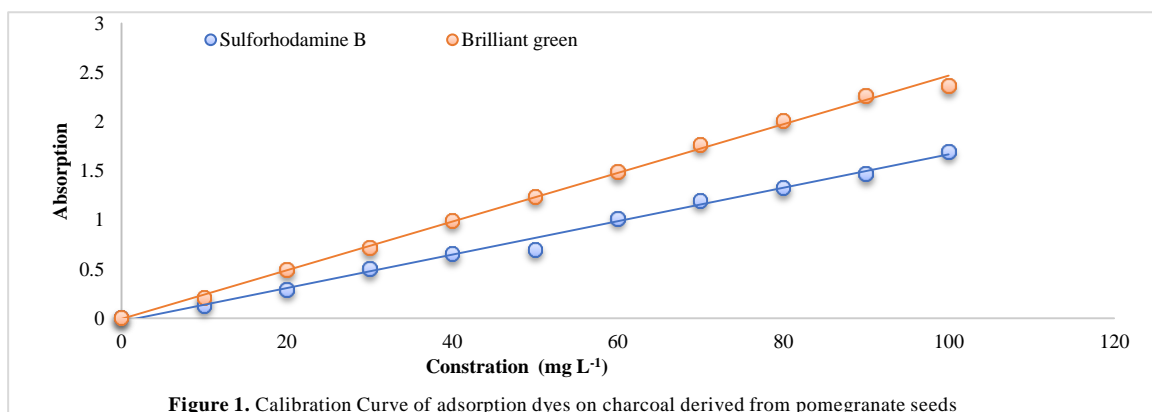


Figure 1. Calibration Curve of adsorption dyes on charcoal derived from pomegranate seeds

Table 1. The general features of used dye

Dyes	Chemical Structure	Molecular weight(g/mol)	$\lambda_{max}(nm)$
Sulforhodamine B		558.6	554
Brilliant green		482.6	628

### Batch adsorption experiments

The adsorption studies were performed in glass flasks with a dye solution stirred continuously at 200 rpm during the experiment. To make a stock solution of 50 mg L, the required amount of dye was dissolved in distilled water and consistent concentrations of solution with appropriate dilutions were obtained. The initial concentration is 1 to 10 mg L, the contact time is 0.5 to 3 hours, the mass of pomegranate seeds is 0.05 to 0.3 g L<sup>-1</sup>, the temperature is 25 to 55°C and the pH range of the solution is 2 to 12. The pH of the solution was adjusted with NaOH (0.1 N) and / or HCl (0.1 N) before measurement using a pH meter. Samples were centrifuged at regular intervals and residue

concentrations were calculated using UV-vis absorption characterization and a method of calibration at the maximum absorption wavelength shown in Table 1. The amount of adsorption was calculated using the following formula [30, 31].

$$Q_e = \frac{(C_0 - C_e)V}{M}$$

## RESULTS AND DISCUSSION

### Structure optimized of dyes

Molecular reactivity diagrams represent the optimization of the molecular structure, including the values of the

reactivity index. Figure 2 indicates the optimized structure of the molecule generated by the Gaussain09W program. Gauss-view06-based reactivity calculations are based on molecular symmetry, a very powerful tool. Molecular optimization can be used to determine that

two molecules have multiple axes of symmetry. Molecules include the asymmetric and nonplane plane and there are two or more symmetrical and plane elements of the molecule.

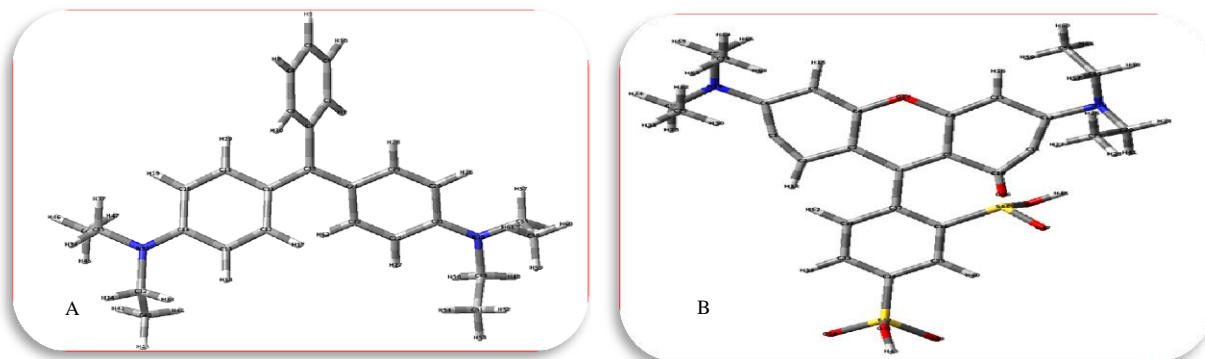


Figure 2. Optimized Structure of Brilliant green dye (A) and Sulfo rhodamine B (B).

### Bond length

The defined bond length between two atoms with two nuclei is approximately the sum of the covalent radii of the two atoms [32]. For covalent bonds, the energy and length of the bond depend on many factors, such as the proximity of electrons, the size of atoms, the differences

in electronegativity, and the overall structure of the molecule. There is a general tendency for shorter bond lengths to have higher bond energies. Similar bond lengths indicate molecular similarity and symmetry (see Figure 3).

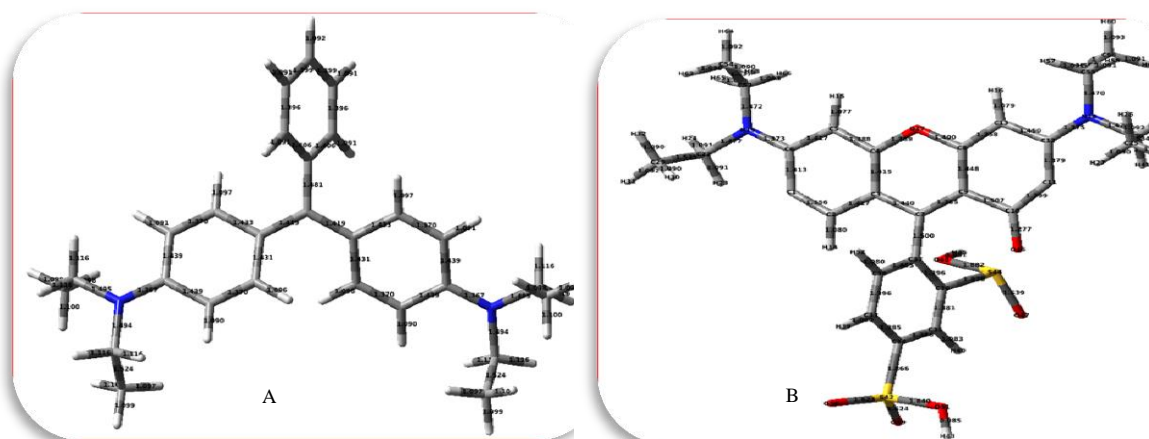


Figure 3. Bond Length of A is Brilliant green dye and B is Sulfo rhodamine B.

### Global reactivity descriptors

#### Energy gap ( $\Delta E_{gap} = E_{HOMO} - E_{LUMO}$ )

The energy gap is vital for influencing the chemical reactivity of dye molecules to adsorption on the adsorbent surface. The obtained results indicate that the sulforhodamine B dye has a lower  $E_{gap}$  ( $E_{gap} = 0.00003$  eV) than the bright green dye with a difference of 0.09062. eV indicates that the sulforhodamine B dye is more reactive than the bright green dye. As a result, the

sulforhodamine B dye is adsorbed first. As shown in Figure 4.

#### Dipole moment ( $\mu$ )

Chemical reactivity may be due to strong molecular polarity. It is clear from the literature that compounds with a higher dipole moment are more active and that

their action greatly increases the removal efficiency. In our case, the higher dipole moment of sulforhodamine B (11.862770D) increased the adsorption between the sulforhodamine B dye and the native clay surface compared to Brilliant Green (1.706186D), which explains the higher adsorption efficiency than sulforhodamine B. Check the experimental results in bright green.

### Study of dyes adsorption

#### The impact of Adsorbent Dosage

Figure 4 shows the adsorption capacity of pomegranate seed carbon obtained from a wastewater sample with pH

= 7 for sorbent doses from 0.05 g to 0.3 g. As a result, the adsorption capacity was very low at the beginning. Thereafter, dose reduction increases the adsorption capacity. This is due to the fact that at first the active site of the adsorbent could not bind effectively to the adsorbate. At large amounts of adsorbent, the active part of the adsorption capacity was almost all the wastewater from the sample. And in the figure, it can be seen that the optimal amount of charcoal obtained from pomegranate seeds is 0.05 g for sulforodamine, which is the maximum adsorption capacity of the dye, and 0.2 g for bright green [33 - 37].

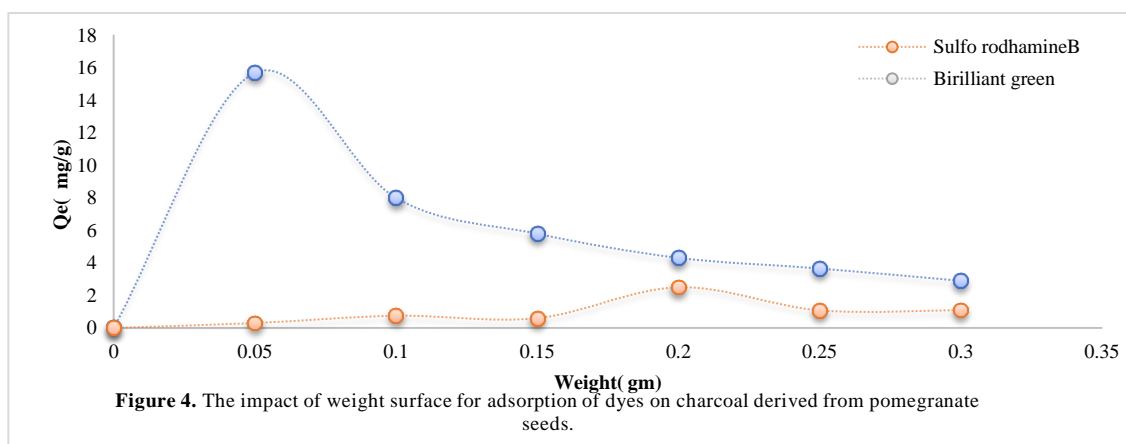


Figure 4. The impact of weight surface for adsorption of dyes on charcoal derived from pomegranate seeds.

#### The impact of initial dye pH

The pH effect of the solutions was studied in the pH range 2-12. The results are indicated in Figure 5. These results show that the high adsorption capacity of sulforhodamine B is improved at PH = 10, but turns light green at pH = 4. These results can be explained by the

fact that the surface of pomegranate seed coal at acidic pH is positively charged [38] and does not contribute to the adsorption of the dye dispersed because of electrostatic repulsion [39,40]. As shown in Figure 5.

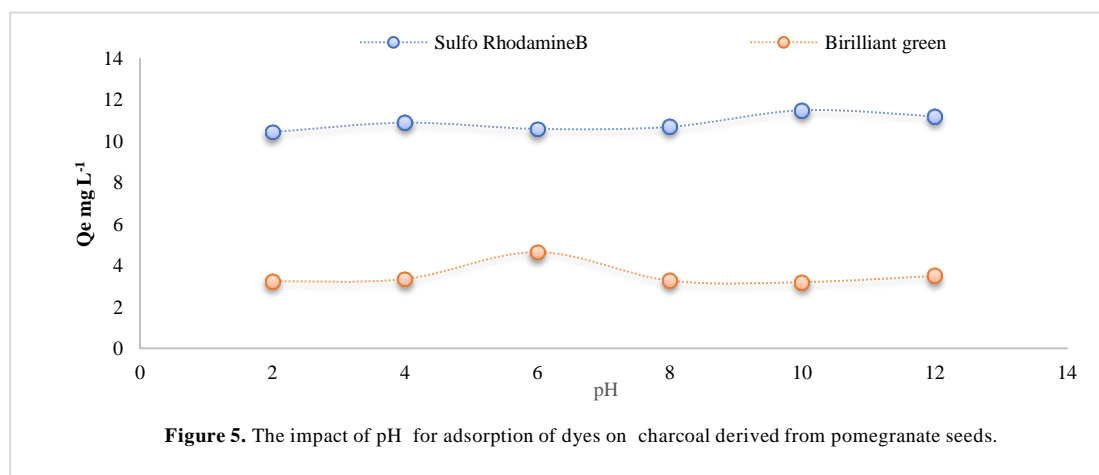


Figure 5. The impact of pH for adsorption of dyes on charcoal derived from pomegranate seeds.

### The impact of temperature

It was conducted that the adsorption capacity decreased with increasing temperature of the solution, indicating that the adsorption mechanism is exothermic and favorable at low temperatures (see Figure 6). The

decrease of the adsorption force with the increase of the temperature may be because of the weakening of the adsorption force between the adsorbent and the active site of the adsorbent [41, 42].

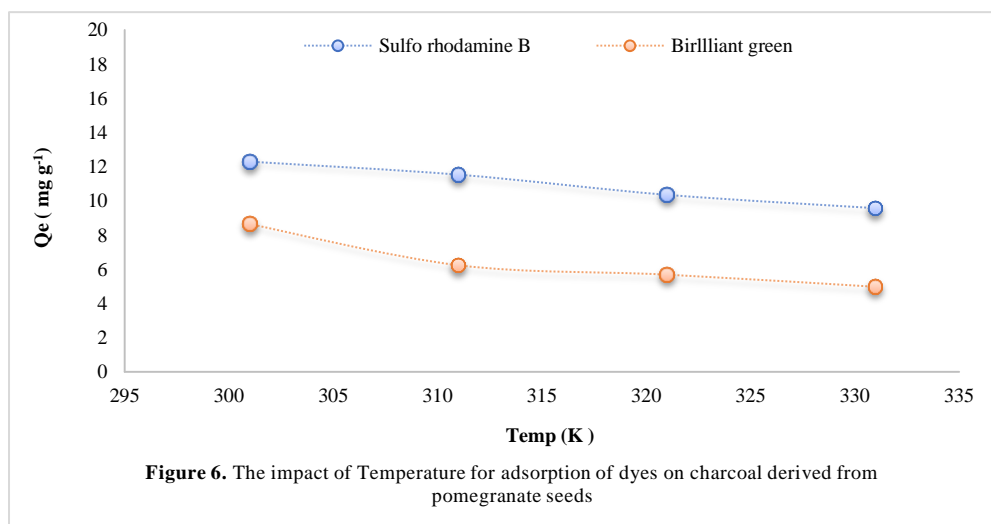


Figure 6. The impact of Temperature for adsorption of dyes on charcoal derived from pomegranate seeds

### Adsorption isotherms

It is necessary to understand the equilibrium adsorption isotherms. Adsorption data are analyzed using the following linear form of the Freundlich and Langmuir isotherms (see the results in Figure 7) [43].

$$\frac{C_e}{q_e} = \frac{1}{q_m \cdot K_L} + \frac{1}{q_m} C_e$$

where  $C_e$  ( $\text{mg L}^{-1}$ ),  $q_e$  ( $\text{mg g}^{-1}$ ),  $K_L$  ( $\text{L mg}^{-1}$ ), and  $q_m$  ( $\text{mg g}^{-1}$ ) are the equilibrium concentration of the adsorbate, the amount adsorbed at equilibrium, the Langmuir constant and the maximum amount of adsorbate, respectively. The linearized Freundlich model is

represented by Equation [44] (see the results in Figure 8):

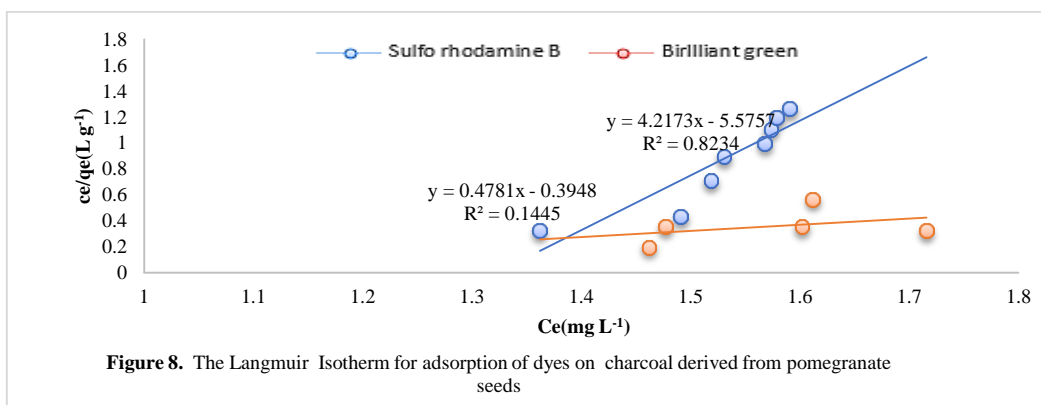
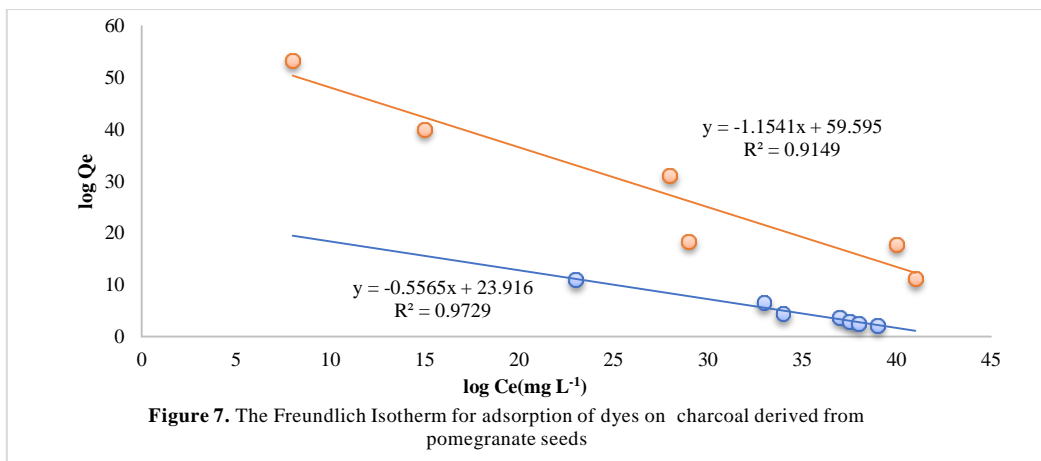
$$\log(q_e) = \log(k_f) + \frac{1}{n} \log(C_e)$$

where  $K_f$  ( $\text{mg g}$ ) and  $n$  are the Freundlich constant related to sorption capacity and the heterogeneity factor, respectively.

As indicated in Table 2, the determination coefficients ( $R^2$ ) are grouped, in comparison with the Freundlich and Langmuir isotherm model, the high correlation coefficient of Freundlich isotherm for both dyes.

Table 2. Isotherm constants for dyes on charcoal from pomegranate seeds.

Dyes	Freundlich			Langmuir		
	Log Kf	1/n-	R2	KL	qm	R2
sulfo rhodamine B	59.595	0.8665	0.9149	1.211	2.0916	0.8234
Brilliant green	23.916	1.7969	0.9729	0.7564	0.2371	0.1445



**Kinetics of adsorption**

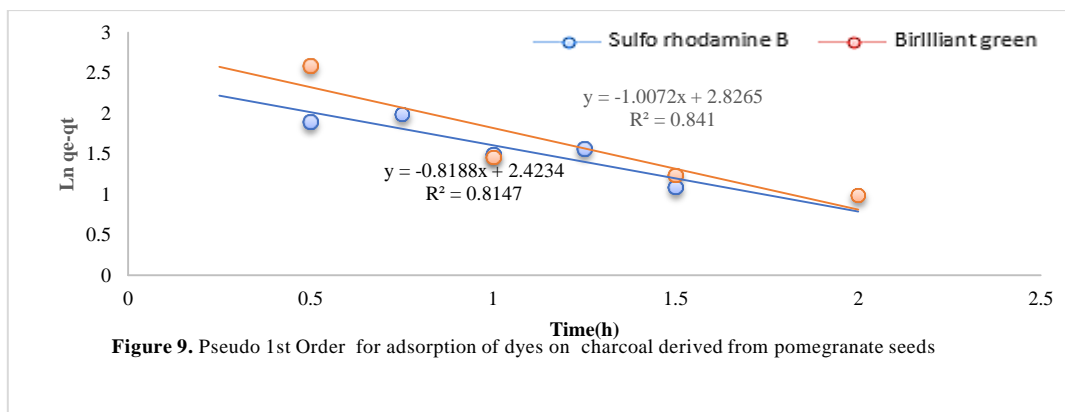
Two kinetics models were used to investigate the adsorption of dyes onto Charcoal from pomegranate seeds such as pseudo-first-order and pseudo-second-order.

**Pseudo-first-order model**

$$\log(q_e - q_t) = \log(q_e) - \frac{k_1}{2.303} t$$

The linear form of pseudo-first-order rate expression is given as:

where  $q_e$  and  $q_t$  are the amount of dye adsorbed on sorbent (mg g) at equilibrium and time  $t$ , respectively,  $k_1$  is the reaction rate constant of pseudo-first-order ( $\text{min}^{-1}$ ) and  $t$  is time (min) [45]. As shown in Figure 9.

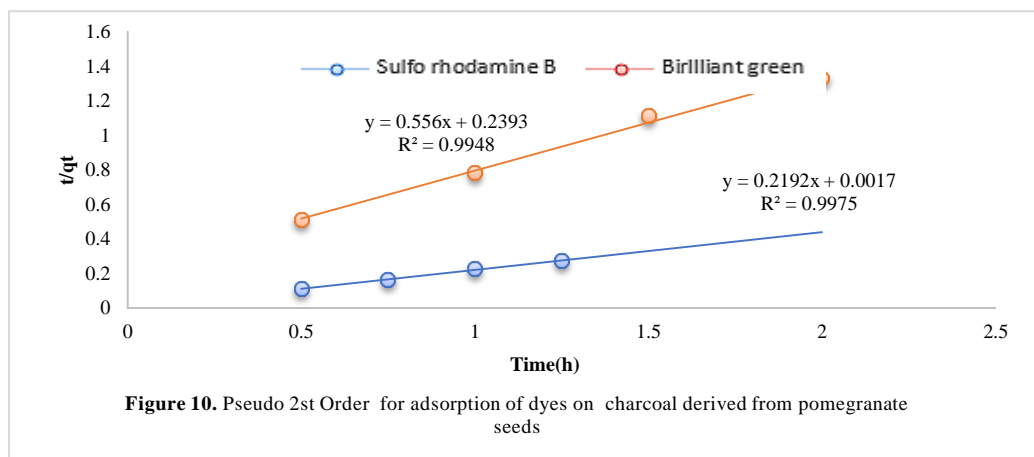


### Pseudo-second-order model

It is necessary to mention that the Pseudo-second-order rate expression reaction model was calculated as

equation [46]. The  $q_e$  and  $k_2$  can be calculated from the slope and intercept of the plot. As shown in Figure 10.

$$\frac{t}{qt} = \frac{1}{K_2 qe^2} + \frac{1}{qe} t$$



### ACKNOWLEDGEMENTS

Not applicable.

### Conflict of interest

The authors declared no conflict of interest.

### REFERENCES

1. Abbas M., Trari M., 2020. Removal of methylene blue in aqueous solution by economic adsorbent derived from apricot stone activated carbon. *Fibers and Polymers*. 21(4), 810-820.
2. Robinson T.M., Marchant R., Nigam P., 2001. Remediation of dyes in textile effluent: A critical review on current treatment technologies with a proposed alternative. *Biores Technol.* 77, 247-255.
3. Khera R.A., Iqbal M., Jabeen S., Abbas M., Nazir A., Nisar J., Tahir M.A., 2019. Adsorption efficiency of Pitpapra biomass under single and binary metal systems. *Surfaces and Interfaces*. 14, 138-145.
4. Abbas M., Adil M., Ehtisham-ul -haque S., Munir B., Yameen M., Ghaffar A., Shar G.A., Tahir M.A., Iqbal M., 2018. *Sci Total Environ.* 626, 1295.
5. Iqbal M., 2016. Vicia faba bioassay for environmental toxicity monitoring: a review. *Chemosphere*. 144, 785-802.
6. Tyagi U., 2020. Adsorption of dyes using activated carbon derived from pyrolysis of vetiveria zizanioides in a fixed bed reactor. *Groundwater for Sustainable Development*. 10, 100303.
7. El Kassimi A., Achour Y., El Himri M., Laamari R., El Hadda M., 2021. Removal of two cationic dyes from aqueous solutions by adsorption onto local clay: experimental and theoretical study using DFT method. *International Journal of Environmental Analytical Chemistry*. 1-22.
8. Mech N., Khemis I.B., Dotto G.L., Franco D., Sellaoui L., Lamine A.B., 2019. Investigation of the adsorption mechanism of methylene blue (MB) on *Cortaderia selloana* flower spikes (FSs) and on *Cortaderia selloana* flower spikes derived carbon fibers (CFs). *Journal of Molecular Liquids*. 280, 268-273.
9. Jawad A.H., Razuan R., Appaturi J.N., Wilson L.D., 2019. Adsorption and mechanism study for methylene blue dye removal with carbonized watermelon (*Citrullus lanatus*) rind prepared via one-step liquid phase H<sub>2</sub>SO<sub>4</sub> activation. *Surfaces and Interfaces*. 16, 76-84.
10. El Kassimi A., Achour Y., El Himri M., Laamari R., El Haddad M., 2021. Removal of two cationic dyes from aqueous solutions by adsorption onto local clay:



experimental and theoretical study using DFT method. International Journal of Environmental Analytical Chemistry. 1-22.

11. Olajire A.A., Giwa A.A., Bello I.A., 2015. Competitive adsorption of dye species from aqueous solution onto melon husk in single and ternary dye systems. International Journal of Environmental Science and Technology. 12(3), 939-950.

12. Khadem L.H., Mageed N.S., 2013. Removal of Azo Compounds from Aqueous Solutions by the Process of Adsorption on Bentonite Surfaces. J Chem and Chem Sci. 3(3), 117-130.

13. Xie H.J., Tan W., Zhang J., Niu H.B., 2011. Adsorption of Methylene Blue from Aqueous Solution onto Peracetic Acid-Modified Loosestrife Powder-A New Adsorbent. In Advanced Materials Research. Trans Tech Publications Ltd. 152, pp. 691-696.

14. Lin Y.Q., Tsai W.T., 2021. Liquid-Phase Removal of Methylene Blue as Organic Pollutant by Mesoporous Activated Carbon Prepared from Water Caltrop Husk Using Carbon Dioxide Activation. Processes 2021. 9, 238.

15. Suárez-García F., Martínez-Alonso A. Tascón J., 2001. Porous texture of activated carbons prepared by phosphoric acid activation of apple pulp. Carbon. 7(39), 1111-1115.

16. Ahmed M.J., Dhedan S.K., 2012. Equilibrium isotherms and kinetics modeling of methylene blue adsorption on agricultural wastes-based activated carbons. Fluid Phase Equilibria. 317, 9-14.

17. Berrios M., Martín M., Martín A., 2012. Treatment of pollutants in wastewater: Adsorption of methylene blue onto olive-based activated carbon. Journal of Industrial and Engineering Chemistry. 18(2), 780-784.

18. Attia A.A., Girgis B.S., Fathy N.A., 2008. Removal of methylene blue by carbons derived from peach stones by H<sub>3</sub>PO<sub>4</sub> activation: Batch and column studies. Dyes and Pigments. 76(1), 282-289.

19. Abbas M., 2020. Experimental investigation of activated carbon prepared from apricot stones material (ASM) adsorbent for removal of malachite green (MG) from aqueous solution. Adsorption Science & Technology. 38(1-2), 24-45

20. Baquero M.C., Giraldo L., Moreno J.C., Suarez-Garcia F., Martinez-Alonso A., Tascón J.M., 2003.

Activated carbons by pyrolysis of coffee bean husks in presence of phosphoric acid. Journal of Analytical and Applied Pyrolysis. 70(2), 779-84.

21. Kyzas G.Z., Lazaridis N.K., Mitropoulos A.C., 2012. Removal of dyes from aqueous solution with untreated coffee residues as potential low-cost adsorbents: Equilibrium, reuse and thermodynamic approach. Chemical Engineering Journal. 189, 148-159.

22. Yagmur E., Ozmak M., Aktas Z., 2008. A novel method for production of activated carbon from waste tea by chemical activation with microwave energy. Fuel. 87(15-16), 3278-3285

23. Valix M., Cheung W.H., McKay G., 2004. Preparation of activated carbon using low temperature carbonization and physical activation of high ash raw bagasse for acid dye adsorption. Chemosphere. 56(5), 493-501.

24. Laine J., Calafat A., Labady M., 1989. Preparation and characterization of activated carbons from coconut shell impregnated. Carbon. 27(2), 191-195

25. Harrache Z., Abbas M., Aksil T., Trari, M., 2019. Modeling of adsorption isotherms of (5, 5'-disodium indigo sulfonate) from aqueous solution onto activated carbon: equilibrium, thermodynamic studies, and error analysis. Desalination and Water Treatment. 147, 273-283.

26. Frisch M.J., Trucks G.W., Schlegel H.B., Scuseria G.E., Robb M.A., Cheeseman J.R., Scalmani G., Barone V., Mennucci B., Petersson G.A., 2010. Gaussian 09, Revision C.01; Gaussian Inc. Wallingford, CT, USA.

27. Dennington R., Keith T., Millam J., 2009. GaussView, Version 5, Semichem Inc. Shawnee Mission, KS.

28. Belghiti M.E., Bouazama S., Echihi S., Mahsoun A., Elmelouky A., Dafali A., Tabyaoui M., 2020. Understanding the adsorption of newly Benzylidene-aniline derivatives as a corrosion inhibitor for carbon steel in hydrochloric acid solution: Experimental, DFT and molecular dynamic simulation studies. Arabian Journal of Chemistry. 13(1), 1499-1519.

29. Geerlings P., Chamorro E., Chattaraj P.K., De Proft F., Gázquez J.L., Liu S., Ayers P., 2020. Conceptual density functional theory: status, prospects, issues. Theoretical Chemistry Accounts. 139(2), 1-18.

30. Boumya W., Khnifira M., Machrouhi A., Abdennouri M., Sadiq M., Acha, M., Barka N., 2021. Adsorption of Eriochrome Black T on the chitin surface: Experimental study, DFT calculations and molecular dynamics simulation. *Journal of Molecular Liquids*. 331, 115706.
31. Sadegh H., Ali G.A., Makhlof A.S., Chong K.F., Alharbi N.S., Agarwal S., Gupta V.K., 2018. MWCNTs-Fe<sub>3</sub>O<sub>4</sub> nanocomposite for Hg (II) high adsorption efficiency. *Journal of Molecular Liquids*. 258, 345-5.
32. Das M.P., Renuka M., Vijaylakshmi J.V., Suguna P.R., 2018. Removal of Methylene Blue by Adsorption Using Fish Scale Chitin. *Nature Environment and Pollution Technology*. 17(3), 993-998.
33. Maruca R., Jo Sunder B., Wightman J.P., 1982. Interaction of heavy metals with chitin & chitosan III Chromium. *J Appl Pol Sci*. 27, 4827-4837.
34. Attia A.A., Girgis B.S., Khedr S.A., 2003. Capacity of activated carbon derived from pistachio shells by H<sub>3</sub>PO<sub>4</sub> in the removal of dyes and phenolics. *J Chem Technol Biotechnol*. 78, 611-619.
35. Dursun A.Y., 2003. The effect of pH on the equilibrium of heavy metal bisorption by *Aspergillus niger*. *Fresenius Environ Bull*. 12, 1315-1322.
36. Kim S.K., Rajapakse N., 2005. Enzymatic reduction and biological activities of chitosan oligosaccharides (COS): A review. *Carboh Pol*. 62, 357-368.
37. Marthur N.K., Narang C.K., 1990. Chitin and Chitosan, versatile polysaccharides from marine animals. *J Chem Ed*. 67, 938-942.
38. Shaban M., Abukhadra M.R., Khan A.A.P., Jibali B.M., 2018. Removal of Congo red, methylene blue and Cr (VI) ions from water using natural serpentine. *Journal of the Taiwan Institute of Chemical Engineers*. 82, 102-116.
39. Lai C.H., Chen C.Y., 2001. Removal of metal ions and humic acid from water by iron-coated filter media. *Chemosphere*. 44(5), 1177-1184.
40. Namal O.O., Kalipci E., 2020. Adsorption kinetics of methylene blue removal from aqueous solutions using potassium hydroxide (KOH) modified apricot kernel shells. *International Journal of Environmental Analytical Chemistry*. 100(14), 1549-1565.
41. Munagapati V.S., Wen H.Y., Vijaya Y., Wen J C., Wen J.H., Tian Z., Raul Garcia J., 2021. Removal of anionic (Acid Yellow 17 and Amaranth) dyes using aminated avocado (*Persea americana*) seed powder: adsorption/desorption, kinetics, isotherms, thermodynamics, and recycling studies. *International Journal of Phytoremediation*. 1-13.
42. Fegousse A., El Gaidoumi A., Miyah Y., El Mountassir R., Lahrichi A., 2019. Pineapple bark performance in dyes adsorption: optimization by the central composite design. *Journal of Chemistry*. (3), 1-11.
43. Langmuir I., 1916. The constitution and fundamental properties of solids and liquids. Part I. Solids. *Journal of the American chemical society*. 38(11), 2221-2295.
44. Freundlich H., 1907. Über die adsorption in lösungen. *Zeitschrift für physikalische Chemie*. 57(1), 385-470.
45. El Kassimi A., Boutouil A., El Himri M., Laamari M.R., El Haddad M., 2020. Selective and competitive removal of three basic dyes from single, binary and ternary systems in aqueous solutions: A combined experimental and theoretical study. *Journal of Saudi Chemical Society*. 24(7), 527-544.
46. Mullick A., Moulik S., Bhattacharjee S., 2018. Removal of hexavalent chromium from aqueous solutions by low-cost rice husk-based activated carbon: kinetic and thermodynamic studies. *Indian Chemical Engineer*. 60(1), 58-71.